ISSN 1330-3651 (Print), ISSN 1848-6339 (Online)
UDC/UDK 534.63:621.396.67]:004.032.26

NEURAL NETWORK BASED ESTIMATION OF RESONANT FREQUENCY OF AN EQUILATERAL TRIANGULAR MICROSTRIP PATCH ANTENNA

Kamil Yavuz Kapusuz, Hakan Tora, Sultan Can

Original scientific paper
This study proposes an artificial neural network (ANN) model in order to approximate the resonant frequencies of equilateral triangular patch antennas. The neural network structure applied here is trained and tested for both single-layer and double-layer antennas. It is shown upon experiment that the resonant frequencies obtained from the neural network are both more accurate than the calculated frequencies by formula and satisfactorily close to the measured frequencies. Results appear to be promising as per the available literature. This paper also may offer more efficient approach to developing antennas of such nature. While the total absolute error of 7 MHz and the average error of 0,09 % are achieved for single-layer antenna, the total absolute and average errors are 49 MHz and 0,07 % for the double-layered antenna, respectively.

Keywords: *microstrip antenna, neural network, resonant frequency*

Procjena rezonantne frekvencije antene s istostraničnom trokutastom mikrostrip osnovom zasnovana na neuronskoj mreži

Izvorni znanstveni rad
U ovom se radu predlaže model umjetne neuronske mreže za procjenu rezonantnih frekvencija antena s istostraničnom trokutastom osnovom. Neuronska mreža primijenjena ovdje uvježbana je i testirana za jednoslojne kao i dvoslojne antene. Eksperiment je pokazao da su rezonantne frekvencije dobivene neuronskom mrežom za obadvije antene točnije od frekvencija izračunatih formulom i da su zadovoljavajuće blizu izmjerenim frekvencijama. Rezultati su obećavajući u odnosu na raspoloživu literaturu. Ovaj rad može također ponuditi učinkovitiji pristup za razvoj takvih antena. Dok je ukupna apsolutna greška od 7 MHz i prosječna greška od 0,09 % dobivena za jednoslojnu antenu; za dvoslojnu antenu je ukupna apsolutna greška 49 MHz, a prosječna greška 0,07 %.

Ključne riječi: *mikrostrip antena, neuronska mreža, rezonantna frekvencija*

1 Introduction

Antennas are one of the most critical elements in wireless communication systems. Researchers today are increasingly paying more attention to the design since an efficient one can provide an efficient wireless system [1, 2]. There are several antenna types, classified according to parameters, such as radiation pattern, gain, and areas of application. Today's communication systems, which require small antenna size, have given rise to development of microstrip patch antennas, themselves commonly used in mobile phones, wireless communication devices and global positioning systems (GPS) [1].

Microstrip antennas, also referred to as patch antennas, are fabricated as printed circuit boards by etching the metal element to a dielectric substance [1, 2]. A typical microstrip antenna consists of a ground on one side and a radiating patch on the other side of the dielectric substrate. This radiating patch is made of conductive elements, such as gold and copper. Microstrip patch antennas can be designed in several shapes, including triangular, rectangular, and circular. Among these, triangular ones are one of the most popular since they have similar radiation patterns to the rectangular ones but are smaller when compared in terms of physical dimension [1]. Due to the advantage in fabrication, they have received more attention. Aside from this, a narrow bandwidth property is an important disadvantage to cope with since designers experience difficulty determining the resonant frequency accurately. There are various studies performed to achieve accurate results regarding resonant frequencies [1, 2]. These models mostly employ the transmission line model (TLM), method of moments (MOMs), and cavity model analysis [1, 3, 4, 5, 6, 15].

In recent years, artificial neural network (ANN) whose structure is inspired by the human brain has been widely used in several fields as well as applications, such as speech recognition, image processing and function approximation. The strengths that include nonlinearity, adaptivity, and input-output mapping have put the spotlight on ANN [2]. As aforementioned, the most widely used models for determining the resonant frequency are summarized as TLM, MOMs, and cavity models. In addition to this, artificial neural networks have emerged as a useful approach for calculating the resonant frequency [2, 7, 8, 14]. When compared to TLM, MOM and cavity model, ANN model not only provides more accurate results but also is faster.

The studies in [2, 3, 8], which are based on neural network models, have all been restricted to a single-layer antenna structure. Within the scope of the present study, however the antenna structure is extended to double-layer geometry with an air gap at the bottom of the substrate layer. Thus, the resonant frequency of our antenna can be set to different values by adjusting the air-gap thickness. The proposed ANN model calculates the resonant frequency of the equilateral triangular patch antenna both with and without an air-gap layer. Our neural computation results are the lowest error in the literature according to our best knowledge [1, 2].

2 Proposed single and double layer antennas

This study is based on two different antenna geometries: single and double. The former has only a thickness of substrate as used in the model, while the latter is designed to have an air-gap layer in addition to

the substrate layer. The air-gap layer yields to tuneable resonant frequency of antenna. As shown in Fig. 1, a double-layer antenna has two layers of substrate. However, it turns into single-layer antenna when the thickness of the air gap layer h_a is set to zero. The shape of the patch is an equilateral triangle with a side length of L. The substrate permittivity and the permeability are indicated as ε_r and μ_r, respectively. The thickness of the substrate is assigned as h_s.

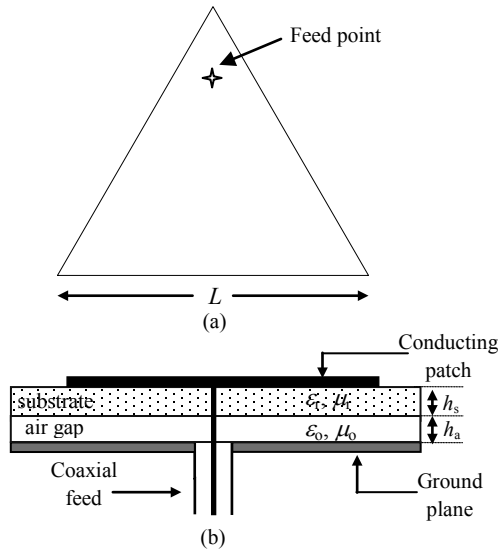

Figure 1 A double-layer antenna (a) Top view (b) Side view

The permittivity and permeability values of the air gap are denoted as ε_0 and μ_0. For both antennas, a coaxial cable is used for feeding and the conductor patch is the radiating part.

3 Determination of resonant frequency

The importance of calculating the resonant frequencies of the microstrip antennas causes an interest to reduce the error of such calculation. Various methods have been proposed in the literature in order to compute the resonant frequencies efficiently. Any antenna's resonant frequency is usually calculated via TLM, cavity model, or MOMs [1]. Since the cavity model results presented in [1] are referred to as the most accurate results for the equilateral triangular microstrip patch antennas, our ANN results are also compared with the cavity model in addition to the other models.

3.1 The resonant frequency of an equilateral triangular patch

The resonant frequency f_r of an equilateral triangular microstrip patch is determined by Eq. (1), which is based on cavity model analysis and curve fitting in [1].

$$f_r = \frac{2c \cdot \sqrt{m^2 + m \cdot n + n^2}}{3 \cdot L_{eff} \cdot \sqrt{\varepsilon_{eff}}}. \quad (1)$$

The m and n represent the mode indexes with mode index coefficient M, which is given in [5, 9]. c is the speed of light in vacuum. L_{eff} is the effective side length of the triangular patch and given by Eq. (3). It depends on the effective side length, r_{eff} of the patch, which is obtained by replacing the triangular patch with a circular one, with a radius r expressed via Eq. (2).

$$r_r = \frac{3L}{2\pi}, \quad (2)$$

where L is the side length of the triangular patch. The fringe field effects occurring around the triangular patch are taken into consideration by such replacement. This replacement is performed in order to place the fringe field effects in computation.

$$L_{eff} = \frac{2\pi \cdot r_{eff}}{3}, \quad (3)$$

r_{eff} is defined by Eq. (4) taken from [1]. As seen from Eq. (4), r_{eff} is a function of total thickness ($h_t = h_s + h_a$), side length L, mode indexes (m, n), and permittivity values.

$$r_{eff} = r \cdot \left(1 + \left(\frac{2h_t}{\varepsilon_{r2} \cdot r \cdot \pi} \right) \cdot \ln \left(\frac{r}{M \cdot h_t \cdot (n+3m)} \right) + 1{,}41\varepsilon_{r2} + 1{,}77 + \frac{h_t}{r} \cdot (0{,}268\varepsilon_{r2} + 1{,}65) \right)^{\frac{1}{2}}. \quad (4)$$

The effective permittivity ε_{eff} is another parameter that varies the resonant frequency of the antenna. It is determined by Eq. (5) in [1].

$$\varepsilon_{eff} = \frac{1}{2} \cdot (\varepsilon_{req} + 1) + \frac{1}{2} \cdot (\varepsilon_{req} - 1) \cdot \left(1 + \frac{12}{W/h_{eq}} \right)^{-\frac{1}{2}}. \quad (5)$$

The equivalent thickness is defined as $h_{eq} = h_s + (h_a/n^{1,2})$ [1]. For single-layer antennas, h_a is set to zero.

3.2 ANN model approach for determination of resonant frequency

The artificial neural networks have recently been used to calculate the resonant frequency of antennas [2, 7, 8]. There exist many available neural network structures [7]. However, multi-layer perceptron (MLP) is one of the most useful network structures finding applications in several fields because it is both simple and accurate [7].

We used a neural network model to calculate the resonant frequency of equilateral microstrip patch antenna with and without air-gap. The neural network needs only six parameters, n, m, L, ε_r, h_s, h_a to compute the resonant frequency. Therefore, there is no need for additional calculations of ε_{eff}, r_{eff}, W, h_{eq}, h_t, L_{eff}, ε_{eff}. Thus, the neural network approach reduces the computational burden.

It should also be noted that a neural network computation could be more accurate in practice than (1) ÷ (5), as it is based on experimentally measured results, effectively interpolating and/or extrapolating from them. In this work, an MLP feed forward back propagation is

employed as a neural network model shown in Fig. 2. The employed MLP network has 3 layers: an input layer, a hidden layer with a sigmoid activation function, and a linear output layer. As seen from Fig. 2, the neural network is fed by the six parameters of the antenna. The resonant frequency f_r is considered as an output of the network.

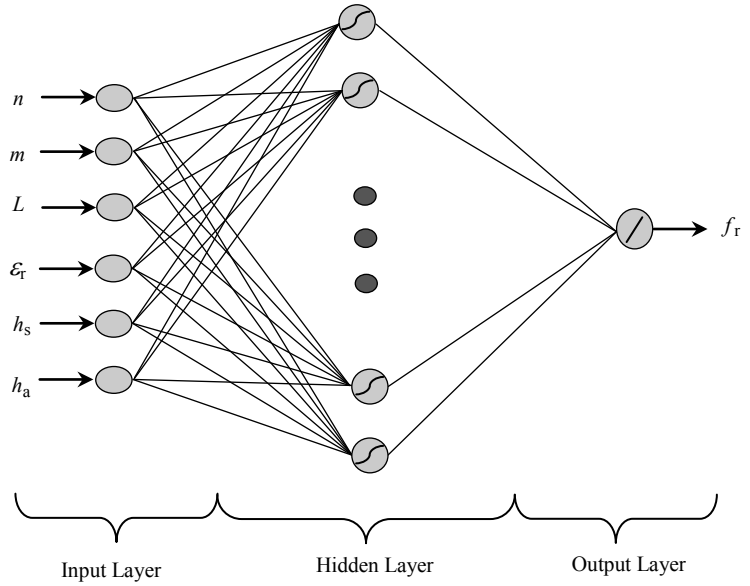

Figure 2 The proposed multi-layer perceptron network structure

In this work, an MLP feed forward back propagation is employed as a neural network model shown in Fig. 2. The employed MLP network has 3 layers: an input layer, a hidden layer with a sigmoid activation function, and a linear output layer. As seen from Fig. 2, the neural network is fed by the six parameters of the antenna. The resonant frequency f_r is considered as an output of the network.

The proposed neural network model approximates the experimentally measured values of resonant frequencies. Those values can be expressed as a function of six antenna parameters by Eq. (6).

$$f_{r_i}^t = f(m_i, n_i, L_i, \varepsilon_{r_i}, h_{s_i}, h_{a_i}). \tag{6}$$

Where t indicates the target and i=1,...N, and N is the number of the examples in the training set of the network. In other words, Eq. (6) is the desired value of the network output. When the network is fully trained, the neural network computes the nearly true resonant frequency as its output. This output can be expressed as a function of its inputs and corresponding desired value given by Eq. (7).

$$f_{r_i}^a = f\left\{m_i, n_i, L_i, \varepsilon_i, h_{s_i}, h_{a_i}; f_{r_i}^t\right\}, \tag{7}$$

where a stands for actual. The absolute difference between the values resulting from Eq. (6) and Eq. (7) is a measure of how well the network meets the measured resonant frequency values. Therefore, this difference is used as a performance criterion for the proposed method given by Eq. (8).

$$error = \left| f\left\{m_i, n_i, L_i, \varepsilon_i, h_{s_i}, h_{a_i}; f_{r_i}^t\right\} - f(m_i, n_i, L_i, \varepsilon_{r_i}, h_{s_i}, h_{a_i}) \right|. \tag{8}$$

The multilayer perceptron is trained by back propagation algorithm. The objective of the training process is to update the synaptic weight $w_{ji}(n)$ so that the output $f_{r_i}^a$ of the neural network matches the desired data $f_{r_i}^t$ as closely as possible. The updated weights are as follows:

$$w_{ji}(n) = w_{ji}(n-1) + \Delta w_{ji}(n), \tag{9}$$

where n is the iteration number and $\Delta w_{ji}(n)$ is the adjustment applied to $w_{ji}(n)$ given by

$$\Delta w_{ji}(n) = \eta \delta_j(n) y_i(n). \tag{10}$$

In Eq. (10), η is the learning rate parameter of the algorithm and y_i is the output of the neuron i. δ_j is the local gradient. The computation of local gradient depends on whether j is an output or a hidden neuron:

$$\delta_j(n) = \begin{cases} \delta_o, & \text{if } j \text{ is output neuron} \quad (11a) \\ \delta_h, & \text{if } j \text{ is hidden neuron,} \quad (11b) \end{cases}$$

where δ_o and δ_h refer to

$$\delta_o = y_i(1-y_i)(d_i - y_i),$$

$$\delta_h = y_i(1-y_i) \sum_{\substack{k \text{ of next} \\ \text{layer}}} \delta_k w_{kj}.$$

In Eq. (11a), d_j and y_j correspond to the desired value of the network output $f_{r\,i}^{t}$ and the actual value of the network output $f_{r_i}^{a}$, respectively. In Eq. (11b), δ_k is local gradient of neuron k in the next layer and w_{kj} is the synaptic weight from neuron k to neuron j.

The study in [14] uses neural network model to estimate the resonant frequencies for a rectangular multilayer antenna with a GaAs substrate. On the other hand, up to this point, the neural network approach has not been used for the calculation of the resonant frequencies of the air-gap loaded triangular double-layer antennas, according to the available literature. Therefore, the proposed neural network model in this paper deals with not only the single-layer, but also the double-layer antennas with an air-gap.

Table 1 The resonant frequencies of an antenna in MHz with L=4,1 cm, ε_r=10,5, h_s= 0,07 cm, h_a= 0 cm

Mode	f_{meas} [3]	$f_{Proposed}$	f_{KG} [4]	f_{SK} [2]	f_{HJ} [5]	f_{GL} [11]	f_{KK} [12]	f_{SD} [6]	f_{GU} [15]
TM_{10}	1519	1519	1501	1526	1498	1494	1490	1494	1511
TM_{11}	2637	2637	2601	2637	2594	2588	2581	2588	2617
TM_{20}	2995	2995	3003	2995	2995	2989	2980	2989	3021
TM_{21}	3973	3973	3972	3973	3962	3954	3942	3954	3997
TM_{30}	4439	4439	4504	4439	4493	4483	4470	4483	4532

Table 2 The resonant frequencies of an antenna in MHz with L=8,7 cm, ε_r=2,32, h_s= 0,078 cm, h_a= 0 cm

Mode	f_{meas} [3]	$f_{Proposed}$	f_{KG} [4]	f_{SK} [2]	f_{HJ} [5]	f_{GL} [11]	f_{KK} [12]	f_{SD} [6]	f_{GU} [15]
TM_{10}	1489	1489	1489	1478	1500	1480	1493	1480	1486
TM_{11}	2596	2596	2579	2596	2599	2564	2585	2564	2573
TM_{20}	2969	2969	2978	2969	3001	2961	3985	2961	2971
TM_{21}	3968	3968	3940	3968	3970	3917	3949	3917	3931
TM_{30}	4443	4443	4468	4443	4501	4441	4478	4441	4457

Table 3 The resonant frequencies of an antenna in MHz with L=10 cm, ε_r=2,32, h_s= 0,159 cm, h_a= 0 cm

Mode	f_{meas} [13]	$f_{Proposed}$	f_{KG} [4]	f_{SK} [2]	f_{HJ} [5]	f_{GL} [11]	f_{KK} [12]	f_{SD} [6]	f_{GU} [5]
TM_{10}	1280	1275	1281	1280	1299	1273	1289	1273	1280
TM_{11}	2242	2242	2219	2242	2251	2206	2233	2206	2217
TM_{20}	2550	2550	2562	2550	2599	2547	2579	2547	2560
TM_{21}	3400	3402	3389	3400	3438	3369	3411	3369	3387
TM_{30}	3824	3824	3843	3829	3898	3820	3868	3820	3840

Table 4 The resonant frequencies of an antenna in MHz with L=1,55 cm, ε_r=2,2, h_s= 0,0508 cm

Mode	h_a / μm	f_{meas} [3]	$f_{Proposed}$	f_{AC} [1]	f_{GS} [10]
TM_{10}	0	8324	8320	8224	8325
TM_{10}	280	9433	9457	9423	9447
TM_{10}	350	9512	9512	9546	9547
TM_{11}	0	14476	14474	14408	14420
TM_{11}	280	16667	16667	16591	16363
TM_{11}	350	16779	16798	16805	16535

Tabs. 1, 2, 3, and 4 illustrate training and test sets obtained from the existing studies in the literature. The first three tables demonstrate the resonant frequencies of single-layer antennas with different antenna parameters, while Tab. 4 shows both single- and double-layer antennas' resonant frequencies. For the proposed neural network, the test data are chosen from Tab. 3 randomly for the modes TM_{10}, TM_{20}, and TM_{21} for the single-layer antenna, while the test data for double-layer antenna is taken from the measured values of the1st, 2nd, 4th, and 6th rows of Tab. 4. The rest of the measured data in those tables have been used for training purposes. Thus, 14 resonant frequencies are used for the training set, and 7 for the test set.

It has been empirically observed that the neural network with one hidden layer consisting of 9 neurons was able to accurately calculate the resonant frequency. In order to decide the number of the neurons in the hidden layer, we train the neural network by increasing the number of the neurons from 2 to 50. As a result, the best performance was achieved with the network with 9 neurons. The learning rate parameter was chosen to be 0,3. The number of the epochs during the training was 5000.

Table 5 Total Absolute Error of resonant frequencies for Tabs. 1, 2 and 3

	$f_{Proposed}$	f_{KG} [4]	f_{SK} [2]	f_{HJ} [5]	f_{GL} [11]	f_{KK} [12]	f_{SD} [6]	f_{GU} [15]
Total Absolute Error / MHz	7	273	23	424	326	349	326	314

Table 6 The resonant frequencies of a single layer antenna with L=10 cm, ε_r =2,32, h_s=0,159 cm, h_a=0

Mode	f_{meas} / MHz [13]	Proposed Model		f_{AC} [1]		f_{GY} [16]		f_{GS} [10]	
		f_r / MHz	*Error* / %	f_r / MHz	*Error* / %	f_r / MHz	*Error* / %	f_r / MHz	*Error* / %
TM_{10}	1280	1275	0,39	1275	0,39	1288	0,63	1285	0,39
TM_{11}	2242	2242	0,00	2221	0,94	2259	0,76	2226	0,71
TM_{20}	2550	2550	0,00	2549	0,04	2610	2,35	2570	0,78
TM_{21}	3400	3402	0,07	3401	0,03	3454	1,59	3400	0,00
TM_{30}	3824	3824	0,00	3854	0,78	3875	1,33	3485	8,87
Average Error / %		0,09		0,44		1,33		2,15	
Total Absolute Error / MHz		7		58		150		102	

Table 7 The resonant frequencies of a double layer antenna with L=1,55 cm, ε_r=2,2, h_s=0,0508 cm

Mode	h_a / μm	f_{meas} / MHz [3]	Proposed Model		f_{AC} [1]		f_{GS} [10]	
			f_r / MHz	*Error* / %	f_r / MHz	*Error* / %	f_r / MHz	*Error* / %
TM_{10}	0	8324	8320	0,04	8224	1,20	8325	0,01
TM_{10}	280	9433	9457	0,24	9423	0,11	9447	0,15
TM_{10}	350	9512	9512	0,00	9546	0,36	9547	0,37
TM_{11}	0	14476	14474	0,01	14408	0,47	14420	0,39
TM_{11}	280	16667	16667	0,00	16591	0,46	16363	1,82
TM_{11}	350	16779	16798	0,11	16805	0,15	16535	1,45
Average Error / %			0,07		0,46		0,70	
Total Absolute Error / MHz			49		314		656	

Tabs. 1, 2, and 3 show the measured and calculated resonant frequencies for different modes of the antennas with different parameters [1-5, 10-15]. In those tables, the second column presents the experimentally measured frequencies and the third column is the computed frequencies from the proposed neural network model. The remaining columns are the resonant frequencies from the literature.

Tab. 4 introduces the resonant frequencies of the antenna structure in Fig. 1 for different modes. The second column indicates the thickness of the air gap.

4 Comparisons of experimental, theoretical, and ANN-derived results

In order to measure the performance of our neural network model, we compared our neural network computed frequencies with the experimental as well as the existing results in the literature. The total absolute error and the average error are defined as performance criteria in the following:

$$Total\ absolute\ error = \sum_{\substack{i:\text{ the number} \\ \text{of modes}}} | f_{meas}^{i} - f_{cal}^{i} | . \tag{12}$$

The error for each mode is determined using Eq. (13).

$$error = \frac{f_{meas} - f_{cal}}{f_{meas}} \times 100, \% \tag{13}$$

where f_{meas} is the experimental results and f_{cal} is the theoretical results for different models and modes.

Tab. 5 lists the overall absolute errors for Tabs. 1, 2 and 3. As seen from Tab. 5, the method applied in this paper appears to be more accurate for single-layer antennas when compared to those in the available literature. Note, for example, that the error of the proposed approach is significantly lower than that of another neural network method, such as [2].

Even though the methods developed in [1, 10, 16] are known to produce the lowest error between values obtained by formulas and measured values, our neural network technique again outperforms those techniques. As clearly seen in Tab. 6, the total absolute error of 7 MHz and average 0,09 % error are achieved. Hence, the validity of the proposed method is proved.

The resonant frequency calculation of double-layer antennas based on the neural network model has not been found in the available literature. Therefore, this case is taken into consideration in this study. The results obtained from the proposed neural network approach and the techniques in [1, 10] are presented in Tab. 7. Clearly, the proposed model here works well in terms of errors when compared to the other two works. Our neural network model is trained by 14 data sets, 12 of which are for single-layer antennas and 2 for double-layer ones. The reason for high error levels in double-layer antennas can be the use of limited training data sets. On the other hand, it is well known that the more input data is used, the more the network generalizes. Thus, the network provides low error for the test data set.

Note that the average error for all modes of single layer antenna is 0,09 % that corresponds to 79,54 % improvement with respect to the lowest error reported thus far in the literature. Similarly, for the double-layer antenna, 84,78 % improvement has been accomplished. Thus, it is confirmed that the proposed neural model optimally approximates the resonant frequencies.

5 Conclusions

In this article, the resonant frequency of an equilateral triangular patch antenna is determined using a multilayer neural network approach. The proposed method is applied to both single- and double-layer antennas. The resonant frequency calculation of a double-layer antenna using a neural network approach is first emerged by this study. It

has been shown that the resonant frequency computed by the proposed neural network approach is much closer to the measured value as compared with the well-known other methods. Hence, a significant error reduction is obtained in ANN.

6 References

[1] Aydin, E.; Can, S. Modified Resonant Frequency Computation for Tunable Equilateral Triangular Microstrip Patch. // The Institute of Electronics, Information and Communication Engineers, 7, 7(2010), pp. 500-505.

[2] Sagiroglu, S.; Guney, K. Calculation of Resonant Frequency for an Equilateral Triangular Microstrip Antenna with the Use of Artificial Neural Networks. // Microwave and Optical Technology Letter, 14, 2(1997), pp. 89-93.

[3] Chen, W.; Lee, K. F.; Dahele, J. S. Theoretical and Experimental Studies of the Resonant Frequencies of Equilateral Triangular Microstrip Antenna. // IEEE Transactions on Antennas Propagation, 40, 10(1992), pp. 1253-1256.

[4] Karaboga, D.; Guney, K.; Karaboga, N.; Kaplan, A. Simple and Accurate Effective Side Length Expression Obtained by Using a Modified Genetic Algorithm for the Resonant Frequency of an Equilateral Triangular Microstrip Antenna. // International Journal of Electronics, 83, 1(2010), pp. 99-108.

[5] Helszajn, J.; James, D. S. Planar Triangular Resonators with Magnetic Walls. // IEEE Transactions Microwave Theory Technology, MTT-26, 2(1978), pp. 95-100.

[6] Singh, R.; De, A.; Yadava, R. S. Comments on 'An Improved Formula for the Resonant Frequency of the Triangular Microstrip Patch Antenna. // IEEE Transactions on Antennas Propagations, 39, 9(1991), pp. 1443–1444.

[7] Karaboga, D.; Guney, K.; Sagiroglu, S.; Erler, M. Neural Computation of the Resonant Frequency of Electrically Thin and Thick Rectangular Microstrip Antennas. // IEE Proc-Microwave Antennas Propagations, 146, 2(1999), pp. 155-159.

[8] Gangwar, S. P.; Gangwar, R. P. S.; Kanaujia, B. K.; Paras, Resonant Frequency of Circular Microstrip Antenna Using Artificial Neural Networks. // Indian Journal of Radio Space & Physics, 37, (2008), pp. 204-208.

[9] Aydin, E.; Can, S. Operating Frequency Calculation of a Shorting Pin-Loaded ETMA. // Microwave and Optical Technology Letter, 54, 6(2012), pp. 1432-1435.

[10] Guha, D.; Siddiqui, J. Y. Resonant Frequency or Equilateral Triangular Microstrip Antenna with and without Air Gap. // IEEE Transactions on Antennas Propagations, 52, 8(2004), pp. 2174-2177.

[11] Garg, R.; Long, S. A. An Improved Formula for the Resonant Frequency of the Triangular Microstrip Patch Antenna. // IEEE Transactions on Antennas Propagation, AP-36, 4(1988), p. 570.

[12] Kumprasert, N.; Kiranon, W. Simple and Accurate Formula for the Resonant Frequency of the Equilateral Triangular Microstrip Patch Antenna. // IEEE Transactions on Antennas Propagations, AP-42, 8(1994), pp. 1178-1179.

[13] Dahele, J. S.; Lee, K. F. On the Resonant Frequencies of the Triangular Patch Antenna. // IEEE Transactions on Antennas Propagations, AP-35, 1(1987), pp. 100-101.

[14] Somasiri, N. P.; Chen, X.; Rezazadeh A. A. Neural Network Modeller for Design Optimisation of Multilayer Patch Antennas. // IEE Proceedings Microwaves, Antennas and Propagation, 151, 6(2004), pp. 514-518.

[15] Guney, K. Resonant Frequency of a Triangular Microstrip Antenna. // Microwave and Optical Technology Letter, 6, 9(1993), pp. 555-557.

[16] Gurel, C. S.; Yazgan, E. New Computation of the Resonant Frequency of a Tunable Equilateral Triangular Microstrip Patch. // IEEE Transactions Microwave Theory Technology, 48, 3(2000), pp. 334-338.

Authors' addresses

Kamil Yavuz Kapusuz
Atilim University
Department of Electrical & Electronics Engineering
Kizilcasar Mahallesi
06836, Incek Golbasi, Ankara, Turkey
kapusuz.kyavuz@gmail.com

Hakan Tora
Atilim University
Department of Electrical & Electronics Engineering
Kizilcasar Mahallesi
06836, Incek Golbasi, Ankara, Turkey
tora@atilim.edu.tr

Sultan Can
Dept. of Electronics Engineering, Ankara University
Tandogan, 06100 Ankara, Turkey
sultancan@ankara.edu.tr